Analyst

FIELD INDUCED DISPLACEMENT REACTIONS WITH PROTON BOUND DIMERS OF ORGANOPHOSPHORUS COMPOUNDS IN A TANDEM DIFFERENTIAL MOBILITY SPECTROMETER

Journal:	*Analyst*
Manuscript ID	AN-ART-05-2021-000783.R1
Article Type:	Paper
Date Submitted by the Author:	04-Jun-2021
Complete List of Authors:	Fowler, Peter; New Mexico State University, Chemistry and Biochemistry Pilgrim, Jacob ; New Mexico State University, Chemistry and Biochemistry Menlyadiev, Marlen; New Mexico State University, Chemistry and Biochemistry Eiceman, Gary; New Mexico State University, Chemistry and Biochemistry; Loughborough Univ., Chemistry

FIELD INDUCED DISPLACEMENT REACTIONS WITH PROTON BOUND DIMERS OF ORGANOPHOSPHORUS COMPOUNDS IN A TANDEM DIFFERENTIAL MOBILITY SPECTROMETER

by

Peter E. Fowler, Jacob Z. Pilgrim, Marlen Menlyadiev, and Gary A. Eiceman
Department of Chemistry and Biochemistry
New Mexico State University
Las Cruces, NM 88003

April 28, 2021
Revised: June 3, 2021

ABSTRACT

Endothermic displacement reactions between proton bound dimers of organophosphorus compounds (OPCs) and isopropanol (IPA) were enabled in air at ambient pressure with tandem differential mobility spectrometry (DMS). Proton bound dimers (M_2H^+) were mobility isolated in purified air with a first DMS stage, mixed with IPA at ≥100 ppm in a middle reactive stage at 106 to 160 Td from a symmetrical 4 MHz waveform, and mobility analyzed in a second DMS stage. Although the enthalpy for displacement of M by IPA in M_2H^+ is unfavorable by +44 to 50 kJ/mole, formation of the heterogenous proton bound dimer, MH^+(IPA) arises from field induced dissociation of M_2H^+ to MH^+ with addition of an IPA. While peak dispersion for M_2H^+ of OPCs is limited to -2.25 to -0.5 V compensation voltage, peaks for MH^+(IPA) were located at -10.5 to -8.25 V through a combination of ion transformation and mobility-based vapor modification. This inaugural use of ion reactions in air at ambient pressure demonstrates that multi-stage sequential processing of ions can improve significantly the analytical performance in a mobility spectrometer.

Key Words: Displacement Reaction, proton bound dimer, organophosphorous compounds, isopropanol, field induced dissociation.

INTRODUCTION

Tandem embodiments of ion mobility analyzers at ambient pressure have emerged in recent years to demonstrate improved selectivity in mobility measurements as ambient pressure analogues to tandem mass spectrometry.[1–6] In drift tubes for these analyzers, ions are mobility selected in a first drift region (or stage), fragmented or decomposed in a middle reactive stage, and mobility analyzed in a second drift stage. Instead of collision induced dissociation in vacuum as with tandem mass spectrometry,[7–9] ions undergo decomposition at ambient pressure with either elevated temperatures[1,2] or electric fields of 100+ Td.[3,4,6] This concept has been demonstrated with three variants in ion mobility spectrometry (IMS) including time-of-drift,[4] differential mobility,[6] and aspirator style analyzers.[1,2] Detection limits and selectivity of response have been improved for chloride adducts of explosives which produce a distinctive nitrate peak in spectra free of ions from other substances and interferences;[2,3] for example, low parts-per-quadrillion were detected in cargo using a combination of ion filtering, thermal decomposition, and mass spectrometer as detector.[2]

A broadened use of IMS for chemical measurements at ambient pressure, perhaps leading to general applications with volatile organic compounds (VOCs) was explored using protonated monomers of oxygen-containing compounds from five chemical families. Field induced fragmentation (FIF) spectra were obtained for these ions using pathways consistent with well-established understandings from mass spectrometry.[10–12] Emphasis was given to the structural content of FIF spectra and to molecular identification by IMS, long considered only a selective trace analyzer with low detection limits for compounds such as organophosphates and organophosphorus compounds (OPCs).[13–15] These have been used as fire suppressants,[16] pesticides,[14,17,18] lubricants for oils in jet engines,[19,20] and chemical warfare nerve agents.[21,22]

The first step of IMS response for OPCs introduces selectivity, even in complex matrices, by favorable reactions with hydrated protons ($H^+(H_2O)_n$), preferentially forming protonated monomer ($M\ H^+(H_2O)_n$) and proton bound dimers ($M_2\ H^+(H_2O)_n$). In the next step of selectivity, differential mobility spectrometers are somewhat limited with proton bound dimers located in a narrow band of compensation voltages. This arises from nearly flat alpha functions for proton bound dimers which are prevalent at vapor concentration ≥ 50 ppb which cause peak overlap near zero compensation voltage with ion masses over ~120 Da.

Improvements in selectivity of response with a tandem DMS analyzer were obtained for VOCs with only ion filtering in two sequential stages when operated with specific combinations of separation voltage and compensation voltage to select for characteristic dispersion plots.[23] Selectivity by DMS/DMS nonetheless was lessened also by overlap of peaks near 0 CV. Ion

peak separation in DMS can be improved using vapor modifiers,[24–27] although ionization chemistry with APCI source can be degraded from percent levels of modifiers. Another possibility, yet undemonstrated with DMS or other IMS methods, is a middle stage where ions could be chemically transformed through field induced reactions such oxidations,[28] derivatizations,[29] and others.[30] In this work, endothermic displacement reactions are used to transform proton bound dimers, $(OPC)_2H^+$ according to Eqs 1 and 2:

$$(OPC)_2H^+ \xrightarrow{E/N} (OPC)H^+ + OPC \quad (1)$$

In this reaction, the field heating from the reactive stage introduces the energy needed to dissociate proton bound dimers and excess levels of reagent (IPA) are used to produce a new ion adduct with the protonated monomer.

$$(OPC)H^+ + IPA \longrightarrow (OPC)H^+IPA \quad (2)$$

In this, neutrals are introduced only in the reactive stage where the new adduct ion ($(OPC)H^+IPA$) is favored by collision frequency with ppm levels of IPA. The objectives in this manuscript are to determine:

a) if the hypothesis can be supported by experimental findings under controlled conditions of a mobility isolated proton bound dimer, heated under control, and adducted in only the reactive stage, and

b) if such facility establishes an architype of multi-step sequential processing of ions in tandem DMS analyzers to increase the capacity of tandem DMS for advanced selectivity.

EXPERIMENTAL

2.1 Instrumentation

Dispersion curves for OPCs in Single stage DMS: Studies on dispersion curves were made using a single stage DMS, a model SVAC instrument (Sionex Corp, Bedford, MA) with the separation region in the DMS 15 mm long x 5 mm wide. The ion source was a 5 mCi ^{63}Ni foil. Carrier gas for this instrument was 0.5 L/min air purified through 13x molecular sieve to a moisture level of 1± 0.2 ppm, as measured by a Moisture Image Series 2 (Panametrics, Inc. Waltham, MA, USA) moisture meter. Temperatures of the carrier gas were measured using thermocouple at the exit port of the DMS analyzer. The SVAC was joined to a model 5890

series II gas chromatograph (Hewlett-Packard Corp, Avondale, PA) equipped with split-splitless injector. The transfer line was a 1.0 m long section of SGE HT5 capillary column (with original dimensions 25mX0.32 mmX0.1μm) from Supelco Analytical (Bellefonte, PA) placed in a heated (100°C) stainless steel transfer line, 30 cm long X 6 mm OD X 3 mm ID tubing. Chromatographic parameters were: carrier gas, nitrogen at 25 cm/s; split ratio, 10:1; injector temperature, 100°C; oven temperature, 100°C.

Reactive multi-stage Tandem DMS: The tandem DMS was made of two plates (Fig. 1) separated by a 0.5 mm Teflon gasket and held under compression in an aluminum frame. The plates were metal-bonded ceramic (REMTEC, Norwood, MA) with 8 mm long × 5 wide mm analyzer stages, a hole for introduction of vapor modifiers in purified air, a 1 mm long × 5 mm wide reactive stage, and 4 mm long × 5 mm wide Faraday plate detectors. The ion source was a 2 mCi Ni-63 foil placed inside a modified stainless-steel union (Swagelok Co., El Paso, TX) attached to the frame holding the plates. Each DMS stage was controlled using custom software and electronics adapted from a handheld DMS called JUNO (ChemRing Sensors and Electronic Systems, Charlotte, NC, USA). Operating parameters of the tandem DMS were: gas temperature at inlet, 65 ± 1 °C; pressure, 660 Torr (8.8 kPa) or number density (N, 1.89×10^{19} molecules cm^{-3} at 65 °C); and linear velocity of gas flow through DMS1 and DMS2 of 6.7 and 10 m s^{-1}, respectively. The temperature gradient in the body of the analyzer was 2 °C. One strip of the reactive stage was provided a symmetric waveform at 4.19 MHz and with amplitudes of 2 to 3 kV peak to peak (106 to 159 Td) at 7.1 to 15.6 W, respectively. These were generated using electronics from GAA Custom Electronics (Kennewick, WA) and the second strip of the reactive stage was at ground potential.

The multi-stage tandem DMS was configured with a model 5890 series II gas chromatograph (Hewlett-Packard Corp, Avondale, PA) as the inlet. It was equipped with a split-splitless injector, a 0.25 μm DB-5 capillary column (15 m long × 0.2 mm ID, Agilent Technologies Inc., Santa Clara, CA), and a transfer line leading to the multi-stage tandem differential mobility spectrometer as detector. The analytical column was joined, using Vu2 Union® Connectors (Restek Corp, Bellefonte, PA), to a 25 cm long aluminum clad SGE HT5 capillary column (0.32 mm ID, 0.1 μm film) from Millipore Sigma (St Louis, MO) kept at 180 °C in the transfer line. A make-up flow for column effluent was 1 L min−1 of air purified through 13× molecular sieve to a moisture of 1 ± 0.5 ppm and monitored using a Moisture Image Series 2 (GE Panametrics, Inc. Waltham, MA). A secondary flow of 0.3 L min−1 of purified air was introduced into a heated flask where a syringe pump could introduce a desired level of vapor modifier prior to injection of

the gas into the instrument through the vapor modifier port. Flow was controlled using mass flow controllers, model 810C-DR-2-VI-SO (Sierra Instruments, Inc. Monterey, CA). Carrier gas for the gas chromatographic column was nitrogen and was purified through in house designed scrubber containing 5 Å molecular sieve and an oxygen/moisture trap Model No: OT3-2 (Agilent Technologies, Santa Clara, CA)

2.2 Reagents and Samples

Seven organophosphorus compounds (OPCs) were obtained from Sigma-Aldrich, Inc. (St Louis, MO, USA) in the highest purity available. These were dimethyl methylphosphonate (DMMP), dimethyl ethylphosphonate (DMEP), diethyl methylphosphonate (DEMP), di-isopropyl methylphosphonate (DIMP), diethyl ethylphosphonate (DEEP), diethyl propylphosphonate (DEPP), and dibutyl butylphosphonate (DBBP). Stock solutions were prepared in dichloromethane (99.7% purity, Alfa Aesar, Tewksbury, MA) at 0.1 to 10 μg μL^{-1} per compound.

2.3 Procedures

Generation of dispersion plots for individual substances. Dispersion plots were generated for individual OPCs using a syringe filled with neat sample and placed into the GC injection port for convenience of entering sample into the DMS analyzer. When vapor flux became constant, the separation voltage (SV) was stepped from 500 to 1500 V in 10 V increments and CV was swept from -43 to +15V in 0.4V steps for each SV step. Stability of OPC concentration over the course of dispersion plot generation was estimated as ±5% by measuring the signal intensity of dimer ion at the beginning and the end of experiment. A composite plot was synthesized computationally by obtaining geometric mean for corresponding data points from SVxCV data matrices of several OPCs.

Ion transformation studies.

General. Solutions of a single OPCs, or a mixture, in solution with CH_2Cl_2 solvent were analyzed by GC-tandem reactive stage DMS using one of several modes including:

Single stage analysis: The first DMS (DMS1, Fig. 1) was inactive (all ion pass, CV=0V; SV=0V) and the second DMS (DMS2) was operated with a separation field of 1350 V (71 Td). Compensation voltage on DMS2 was scanned from -15 to 5 V (0.80 to 0.27 Td) at 0.2 V per step. The reactive stage was inactive.

Mobility selection of Ions: The first DMS (DMS1, Fig. 1) was set to particular pair of CV and SV at separation field always below that of DMS2 and thus is able to mobility isolate acting as an ion filter. Ions are characterized by scanning CV in DMS2. The reactive stage was inactive.
Field induced fragmentation of ions in reactive stage: Ions were mobility filtered using DMS1 and heated in the electric field in the reactive stage. Separation voltages were set and compensation voltage was scanned in DMS2 as in mobility selection of ions.
In all modes, purified air was used to sweep ions through the tandem analyzer and the middle stage was provided a flow of purified air or ≥100 ppm isopropanol in purified air.

Influence of Field Strength: The effect of field strength of the reactive middle stage was studied by varying the field strength applied to the reactive stage, both in clean gas conditions and with the IPA modifier. In this experiment the proton bound dimer of each OPC was isolated in DMS1 and passed to the reactive stage where the field was varied from 106 to 160 Td. Extent of ion transformation and product ions were then characterized in DMS2.

Influence of vapor concentration: Vapor concentrations of IPA in the purified gas stream were tested from 100 to 30,000 ppm of IPA. The instrument was operated with sequential ion processing where the proton bound dimer of DMMP was selected in purified air in DMS1, passed to the vapor modifier stage where IPA was added, then passed through the reactive stage at 160 Td and characterized in DMS2. DMMP was characterized for the IPA vapour concentrations of 0, 100, 250, 500, 750, 1k, 5k, 10k, 20k, and 30k ppm.

Computational Calculation of Reaction Enthalpies.
Enthalpies for reactions corresponding to dissociation of M2.H+ and subsequent association with water or IPA were calculated using Gaussian 09 (Gaussian, Inc., Wallingford CT, 2009) using DFT density functional B3LYP with the 6-311+G(d,p) basis set.

RESULTS AND DISCUSSION

Dispersion plots for OPCs in DMS

Dispersion plots for each of six OPCs are shown as a composite in Fig. 2 where individual plots for proton-bound dimers (M_2H^+) and protonated monomers ($MH^+(H_2O)_n$) exhibit distinctive

patterns which arise from the field dependence of mobility coefficients as described by alpha functions, α(*E/N*), in Equation 3:

$$K(E/N) = K_o [1 + \alpha(E/N)] \quad (3)$$

where α(*E/N*) is a function for the influence of extremes for the asymmetric field on mobility coefficients. The composite plots show two regions (for SV from 600 to 1500 V) including:

a. that for proton bound dimers with CV values from zero to 6V, and

b. that for protonated monomers with CV values from -5 to 2 V, for protonated monomers.

Also shown in Fig. 2 is the dispersion plot for the reactant ions or $H^+(H_2O)_n$ which trends from 0 V to -20 V over the range of SVs.

These dispersion plots are consistent with prior studies[31] of OPCs by DMS where the proton bound dimers in purified air exhibit negative alpha functions (Eq. 3); i.e., reduced mobility coefficients decrease with increased E/N as the influence at field extremes of ion hydration-dehydration lessens with increased ion mass. In contrast, protonated monomers exhibit largely positive alpha functions for SVs from 0 to ~1300 V. Even for these relatively smaller ions, a slight negative alpha function occurs above 1300 V since ions under strong field heating are extensively declustered even during low fields. A practical consequence of peak locations in CV-SV space is that protonated monomers are weakly resolved among OPCs while proton bound dimers exhibit poor capacity for ion separation and particularly analytical specificity against matrix interferents which often are located at or near 0 V.

Mobility isolation of proton bound dimer and field induced dissociation

A contour plot of ion intensity, retention time, and compensation voltage from the GC-DMS determination of DMMP is shown in Fig. 3 (top frame) where the tandem analyzer was operated as a single stage DMS. At times before elution of DMMP, only the hydrated proton at -9.8V compensation voltage is seen. At the elution time for DMMP (48 to 55 s), intensity of the hydrated proton is reduced and intensity increases for peaks of protonated monomer (CV of -2.5V), and proton bound dimer of DMMP (CV of 1.2 V). This occurs stepwise throughout the chromatographic elution profile through Equations 4 and 5:

$$H^+(H_2O)_n + DMMP \text{ <--------> } (DMMP)H^+(H_2O)_{n-y} + yH_2O \quad (4)$$

$$(DMMP)H^+(H_2O)_x + DMMP \text{ <--------> } (DMMP)_2H^+ + xH_2O \quad (5)$$

where formation of proton bound dimer (Eq. 5) *increases with a decreased intensity* of protonated monomer. At retention times after the elution peak maximum, intensity decreases of

proton bound dimer and intensity increases briefly for protonated monomer. Near the end of the elution profile, intensity also decreases for protonated monomer.

The proton bound dimer can be mobility selected and filtered by tandem DMS as shown in Fig. 3 (middle frame). Consequently, neither hydrated protons or protonated monomer were passed into the reactive, or the second DMS, stage and transmission efficiency for proton bound dimer of DMMP was 70%. When the mobility selected ion was dissociated with E/N of 155 Td using a 4.19 MHz waveform (Fig. 3, bottom frame), the dissociation yield was >90% of original proton bound dimer and overall transmission of the proton bound dimer in DMS1 was ca. 63%.

These results demonstrate that proton bound dimers can be mobility-isolated and dissociated with an increase of signal-to-noise (chemical) by excluding other ions and analytical space is increased slightly with an increased displacement in compensation voltage. This was observed for all OPCs where increases in ion mass resulted in improved transmission efficiency, lesser percent dissociation, and lesser displacement in compensation voltage.

Ion transformation with vapour modifier in reactive middle stage

A mobility spectrum for DMMP at maximum chromatographic elution is shown in Figure 4 for the mobility isolated $(DMMP)_2H^+$ and $(DMMP)H^+(H_2O)_{n-y}$ which arises from the dissociation of $(DMMP)_2H^+$ in the reactive stage of the tandem DMS analyzer. Compensation voltages were 1.2 V for $(DMMP)_2H^+$ and -2.25 for $(DMMP)H^+(H_2O)_{n-y}$ at 0 ppm vapour concentration for IPA. When [IPA] was increased to 100 ppm (see Fig. 4, legend), three peaks can be seen and include the $(DMMP)_2H^+$, $(DMMP)H^+(H_2O)_{n-y}$ and a new peak, at -4 CV. At vapour concentrations of 250 to 750 ppm, this new peak is displaced in compensation voltage to -10.0 V with loss of intensity for $(DMMP)H^+(H_2O)_{n-y}$. At 750 and 1000 ppm for IPA, only the $(DMMP)_2H^+$ at 1 CV and the new ion are seen in the spectra. The appearance of this new ion and a dispacement in compensation voltage can be attributed to 1) transformation of $(DMMP)_2H^+$ to protonated monomer and 2) a subsequent formation of a heterogenous proton bound dimer $(DMMP)H^+(IPA)$ as in Equation 6:

$$(DMMP)H^+ + IPA \quad \text{----------}> \quad (DMMP)H^+(IPA) \qquad (6)$$

This heterogenous proton bound dimer should be displaced significantly in compensation voltage from $(DMMP)_2H^+$ due to lesser ion mass, and increased alpha functions (Eq. 3) with vapor modifiers. Ion masses are 249 Da for $(DMMP)_2H^+$ and 185 Da for $(DMMP)H^+(IPA)$ and the close spacing between $H^+(IPA)_x$ and $(DMMP)H^+(IPA)$ suggests a mass of 181 Da for $H^+(IPA)_x$ where x =3. While an intermediate ion $(DMMP)H^+(H_2O)_n$ might exist briefly in the reactive stage of the tandem DMS, the lifetime for this transition species should be

comparatively brief with [IPA] at 100 to 1000 ppm compared to [H_2O] at 1 to 5 ppm and an ion neutral collision every ~100 ps.

Displacement Reactions and Other OPCs

The influences of ion transformation and the selectivity of mobility isolation of ions are shown in Fig. 5 for three OPCs isolated chromatographically and from characterization using the reactive stage tandem DMS. In Fig. 5 (top frame), the DMS was operated as a single stage analyzer and proton bound dimers can be seen for OPCs with elution times of 48 s, DMMP; 145 s, DEMP; and 220s, DEEP. In this measurement, IPA was introduced into the reactive stage which was inactive (no E/N applied). The hydrated proton seen at -10V in Figure 3 (top frame) was converted to $H^+(IPA)_x$; with a compensation voltage now displaced slightly to -10.5 V and with an increased bandwidth (>4 V at baseline compared to ~2.2 V for $H^+(H_2O)_n$). Some distortion in the pattern for $H^+(IPA)_3$, can be seen during the elution of an OPC on the front and tail of the chromatographic band (see below).

When proton bound dimers were mobility isolated and passed into the reactive stage without E/N, the $H^+(IPA)_x$ was removed (Fig. 5 middle frame) and $(OPC)_2H^+$ were visible on a baseline largely free of other ions. The ion abundances for $(OPC)_2H^+$ peak were lessened by some losses during mobility isolation in DMS 1. When E/N was applied in the reactive stage $(OPC)_2H^+$ species were dissociated and formed $(OPC)H^+(IPA)$ as in Eq. 6 (Fig. 5, bottom frame). Percent conversion to $(OPC)H^+(IPA)$ under this set of conditions was roughly 100% DMMP, 50% DEMP; and 20% DEEP and was controlled largely by the dependence of dissociation efficiency on ion size. Benefits in displacement of peaks of OPCs from matrix interferences seen commonly at 0 V in compensation voltage should result in improved selectivity of response with IPA modified ions. The OPCs in this study are partially separated in compensation voltage with differences of 1.8 V between DMMP and DEMP and 0.6 V between DEMP and DEEP for peak width half height of ~2.2 V. In future efforts to employ a reactive stage tandem DMS in analysis of OPC mixtures, separation voltage could be increased to improve separation of $(OPC)H^+(IPA)$ species.

Faintly visible in Fig. 5 (middle frame) is the presence of $(OPC)H^+(IPA)$ even without E/N in the middle stage. This is attributed to fringe fields on $(OPC)_2H^+$ leaving DMS1 or entering DMS2 with elevated [IPA]. Such fringe fields are also visible as peaks partially resolved on the ion trace for $H^+(IPA)_3$ in Fig. 5 (top frame). Control studies showed that intensities of these ions were proportional to separation voltages and undetected below ~100 Td in DMS1. The

increase in peak separation in Fig. 5 (bottom frame) exceeded that for proton bound dimers in Figure 2 and was obtained with control of gas purity for ionization.

Influence of Field Strength on Extent of Displacement Reaction

Spectra for DMMP, DEMP, and DEEP with IPA are overlaid with waveform amplitudes from 0 to 3 kV peak-to-peak (0 to 159 Td) in the reactive stage. In these spectra, proton bound dimers are located near 0V in compensation voltage for each of the three OPCs and field generated ions from the displacement reaction are located at CV values characteristic of each OPC. Intensities for these new ions, $(OPC)H^+(IPA)$, are increased with increased E/N in the reactive stage as the intensity for the proton bound dimer decrease. Since transmission efficiencies in DMS analyzers are based on ion mass, charge is not conserved, and peak areas of $(OPC)H^+(IPA)$ and $(OPC)_2H^+$ cannot be balanced directly with high accuracy. Nonetheless, the *conversion efficiency* based on peak intensity of $(OPC)_2H^+$ at maximum E/N in Fig. 6 is >90% for DMMP, 50% for DEMP, and 35% for DEEP.

Computational Models for Reactions

Formation enthalpies of ions of $(OPC)H^+$(neutral) where the neutral could be water, IPA, or the OPC are shown in Table 1 from DFT calculations using Gaussian software. These can be used to calculate reaction enthalpies (ΔH_{rxn}) for the net reaction shown in Eq. 7. The ΔH_{rxn} for the three OPCs is energetically unfavorable with a range of 44 to 51 kJ/mol demonstrating that the displacement reactions with DMMP, DEMP, and DEEP are unlikely to occur spontaneously.

$(OPC)_2H^+ + IPA \text{ ----------> } (OPC)H^+(IPA) + OPC$ 7

This is consistent with proton affinities of DMMP (895 kJ/mole), DEMP (911 kJ/mol), IPA (793 kJ/mol), and water (697 kJ/mol) and matches the experimental results absent field activation in the reactive stage (Fig 5, top frame). In contrast to this, the reaction in Equation 7 can be driven right by dissociation of proton bound dimers using electric field activation at or above 143 kJ/mol in Equation 8.

$(OPC)_2H^+ \xrightarrow{E/N} (OPC)H^+ + OPC \quad 143 \text{ kJ/mol}$ 8

Subsequent association of the protonated monomer with IPA occurs exothermically in Eq. 9.

$(OPC)H^+ + IPA \text{ ----------> } (OPC)H^+(IPA) \quad -96 \text{ kJ/mol}$ 9

The net process given in Eq. 7, an energetically unfavorable reaction, can be driven by the reactive stage heating to enable formation of a ion not available in other IMS drift tubes.. While dissociation of the dimer in the volume of the reactive stage might result in adduct formation with OPC recently removed or with unreacted OPC passed from the ion source, the vapour concentrations of OPCs in the experiments were estimated at 60 ppb at peak maximum during chromatographic elution. Vapour concentration of water and IPA by comparison were 1 to 10 ppm and 100 to 10000 ppm, respectively. Once dissociated to $(OPC)H^+$ by ion heating in the reactive stage, formation of $(OPC)H^+(IPA)$ is favored by collisional statistics by 100 to 1000X against water and by >150,000 for OPCs within the residence times of ~1 ms in the reactive stage.

CONCLUSIONS

Improvements in selectivity of response with tandem DMS methods compared to single stage DMS analyzer have been increased further through the incorporation of a reactive stage which has been used to activate enable enthalpically unfavorable reactions. In studies here, a displacement reaction was demonstrated to address a practical limitation of single stage DMS, peak separation of proton bound dimers of organophosphorus compounds. Although displacement of an OPC by IPA in $(OPC)_2H^+$ is unachievable in other mobility devices, reactive stage tandem DMS measurements provided yields of 30 to 90% without interferences from ions other than the precursor and product ions. The concept of ion transformation in reactive stages at ambient pressure is presented as a template for other ion reactions such as oxidations and derivatizations. Such reactions may be conveniently planned and controlled with reagents at ambient pressure in air or nitrogen.

AUTHOR CONTRIBUTIONS

Peter Fowler: Data Curation, Investigation, Methodology, Validation, Project administration, Supervision, Visualization, Writing

Gary Eiceman: Conceptualization, Funding acquisition, Resources, Supervision, Writing

Jacob Pilgrim: Investigation, Validation, Visualization

Marlen Menlyadiev: Conceptualization, Writing

ACKNOWLEDGEMENTS

This work was derived from discoveries by Hossein Shokri, Dedeepya Pasupuleti, and Sanna Holopainnen and their contributions are gratefully acknowledged. This work was based upon work supported by the National Science Foundation under award no. CHE-1306388 and award no. IIP-1827525. Insights and discussions with Prof. John Stone, Queens Univ., Ontario, concerning ion dissociation are also gratefully acknowledged.

REFERENCES

1 M. Amo-González, I. Carnicero, S. Pérez, R. Delgado, G. A. Eiceman, G. Fernández De La Mora and J. Fernández De La Mora, *Anal. Chem.*, 2018, **90**, 6885–6892.

2 M. Amo-González, S. Pérez, R. Delgado, G. Arranz and I. Carnicero, *Anal. Chem.*, 2019, **91**, 14009–14018.

3 U. Chiluwal, G. Lee, M. Y. Rajapakse, T. Willy, S. Lukow, H. Schmidt and G. A. Eiceman, *Analyst*, 2019, **144**, 2052–2061.

4 H. Shokri, M. Vuki, B. D. Gardner, H. C. Niu, U. Chiluwal, B. K. Gurung, D. B. Emery and G. A. Eiceman, *Anal. Chem.*, 2019, **91**, 6281–6287.

5 H. Shokri, E. G. Nazarov, B. D. Gardner, H.-C. Niu, G. Lee, J. A. Stone, N. Jurado-Campos and G. A. Eiceman, *Anal. Chem.*, 2020, **92**, 5862–5870.

6 P. E. Fowler, J. Z. Pilgrim, G. Lee and G. A. Eiceman, *Analyst*, 2020, **145**, 5314–5324.

7 D. D. Fetterolf and R. A. Yost, *Int. J. Mass Spectrom. Ion Phys.*, 1982, **44**, 37–50.

8 R. C. Burnier, R. B. Cody and B. S. Freiser, *J. Am. Chem. Soc.*, 1982, **104**, 7436–7441.

9 M. J. Haas and A. G. Harrison, *Int. J. Mass Spectrom. Ion Process.*, 1993, **124**, 115–124.

10 J. A. Herman and A. G. Harrison, *Can. J. Chem.*, 1981, **59**, 2133–2145.

11 M. L. Sigsby, R. J. Day and R. G. Cooks, *Org. Mass Spectrom.*, 1979, **14**, 273–280.

12 S. B. Hawthorne and D. J. Miller, *Appl. Spectrosc.*, 1986, **40**, 1200–1211.

13 T. Satoh, S. Kishi, H. Nagashima, M. Tachikawa, M. Kanamori-Kataoka, T. Nakagawa, N. Kitagawa, K. Tokita, S. Yamamoto and Y. Seto, *Anal. Chim. Acta*, 2015, **865**, 39–52.

14 M. T. Jafari, *Talanta*, 2006, **69**, 1054–1058.

15 G. A. Eiceman, W. Yuan-Feng, L. Garcia-Gonzalez, C. S. Harden and D. B. Shoff, *Anal. Chim. Acta*, , DOI:10.1016/0003-2670(94)00668-C.

16 O. P. Korobeinichev, A. G. Shmakov, V. M. Shvartsberg and S. A. Yakimov, *Study of Fire Suppression Effectiveness of Organophosphorus Compounds and Compositions on Their Base*, 2005.

17 E. Bunert, B. Bernhold, J. N. Woidtke, M. Sehlmeyer and S. Zimmermann, *J. Chromatogr. A*, 2019, **1606**, 460384.

18 D. Gallart-Mateu, S. Armenta and M. de la Guardia, *Talanta*, 2016, **161**, 632–639.

19 D. Megson, X. Ortiz, K. J. Jobst, E. J. Reiner, M. F. A. Mulder and J. C. Balouet, *Chemosphere*, 2016, **158**, 116–123.

20 K. Solbu, H. L. Daae, R. Olsen, S. Thorud, D. G. Ellingsen, T. Lindgren, B. Bakke, E. Lundanes and P. Molander, *J. Environ. Monit.*, 2011, **13**, 1393–1403.

21 M. Maziejuk, M. Ceremuga, M. Szyposzyńska, T. Sikora and A. Zalewska, *Sensors Actuators, B Chem.*, 2015, **213**, 368–374.

22 W. E. Steiner, W. A. English and H. H. Hill, *Anal. Chim. Acta*, 2005, **532**, 37–45.

23 M. R. Menlyadiev and G. A. Eiceman, *Anal. Chem.*, 2014, **86**, 2395–2402.

24 B. B. Schneider, E. G. Nazarov and T. R. Covey, 2012, 141–150.

25 L. C. Rorrer and R. A. Yost, *Int. J. Mass Spectrom.*, 2015, **378**, 336–346.

26 G. A. Eiceman, E. V. Krylov, N. S. Krylova, E. G. Nazarov and R. A. Miller, *Anal. Chem.*, 2004, **76**, 4937–4944.

27 E. Waraksa, U. Perycz, J. Namiesnik, M. Sillanpaa, T. Dymerski, M. Wojjtowicz and J. Puton, *TrAC - Trends Anal. Chem.*, 2016, **82**, 237–249.

28 A. L. Pilo, J. Bu and S. A. McLuckey, *J. Am. Soc. Mass Spectrom.*, 2016, **27**, 1979–1988.

29 M. Fu, P. Duan, S. Li, R. J. Eismin and H. I. Kenttämaa, *J. Am. Soc. Mass Spectrom.*, 2009, **20**, 1251–1262.

30 R. D. Espy, M. Wleklinski, X. Yan and R. G. Cooks, *TrAC - Trends Anal. Chem.*, 2014, **57**, 135–146.

31 N. Krylova, E. Krylov, G. A. A. Eiceman and J. A. A. Stone, *J. Phys. Chem. A*, 2003, **107**, 3648–3654.

Table 1 Enthalpies of reaction in kJ/mol for each OPC with itself, water, or isopropyl alcohol to form ions of the form $(OPC)H^+$(neutral).

Neutral	DMMP	DEMP	DEEP
OPC	-141	-147	-142
H_2O	-80	-85	-84
IPA	-97	-101	-91

LIST OF FIGURES

1. Plate for reactive stage tandem DMS including port for introduction of vapor reagent. Ions are delivered to DMS1 in a purified air atmosphere where the reagent ion is $H^+(H_2O)_n$ with a distribution of n between 3 and 4. The reactive stage is formed in the volume between two plates with a 1 mm wide strip. This precedes DMS2 in sequential processing of ions.
2. Composite plot of dispersion curves for ions from six OPCs as individual vapours in purified air at 80°C. Compounds included DMMP, DMEP, DIMP, DEEP, DEPP, and DBBP.
3. Topographic plot of ion intensity, retention time, and compensation voltage for three modes of measurement of DMMP with a single DMS stage (top), using mobility isolation of proton bound dimer in DMS1 (middle) and field induced dissociation of isolated proton bound dimer to protonated monomer (bottom) in purified air without IPA vapours.
4. Spectra for mobility selected proton bound dimer of DMMP with electric fields applied to the reactive stage for several vapor concentrations of IPA.
5. Topographic plot of ion intensity, retention time, and CV for DMMP, DEMP, and DEEP in 10k ppm IPA in purified air using single DMS stage (top), mobility isolated of proton bound dimers (middle) and electric fields applied to the reactive stage (bottom).
6. Spectra from electric field promoted reactions for DMMP, DEPM, and DEEP in IPA at waveform amplitudes 0 to 3000 V (0 to 159 Td).

Figure 1. Fowler, et al

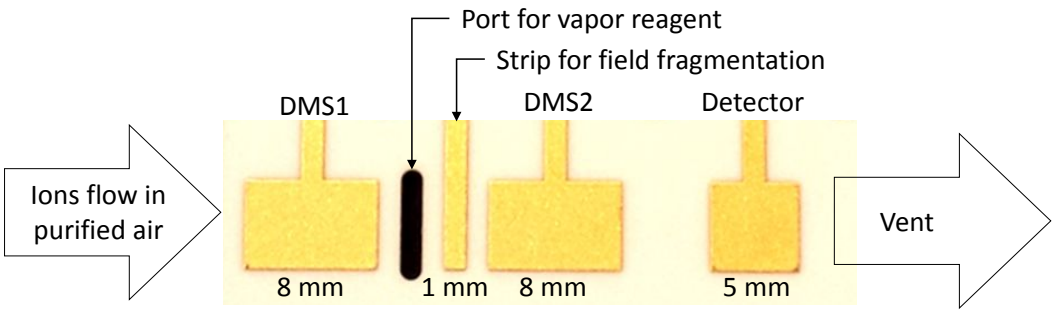

Figure 2. Fowler, et al.

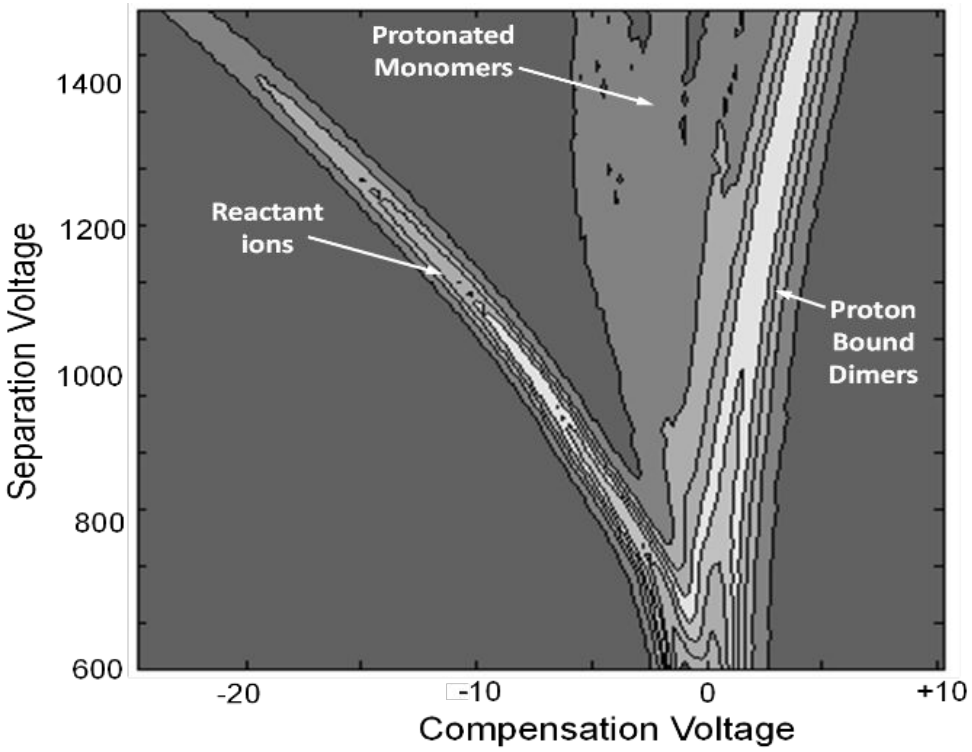

Figure 3. Fowler, et al

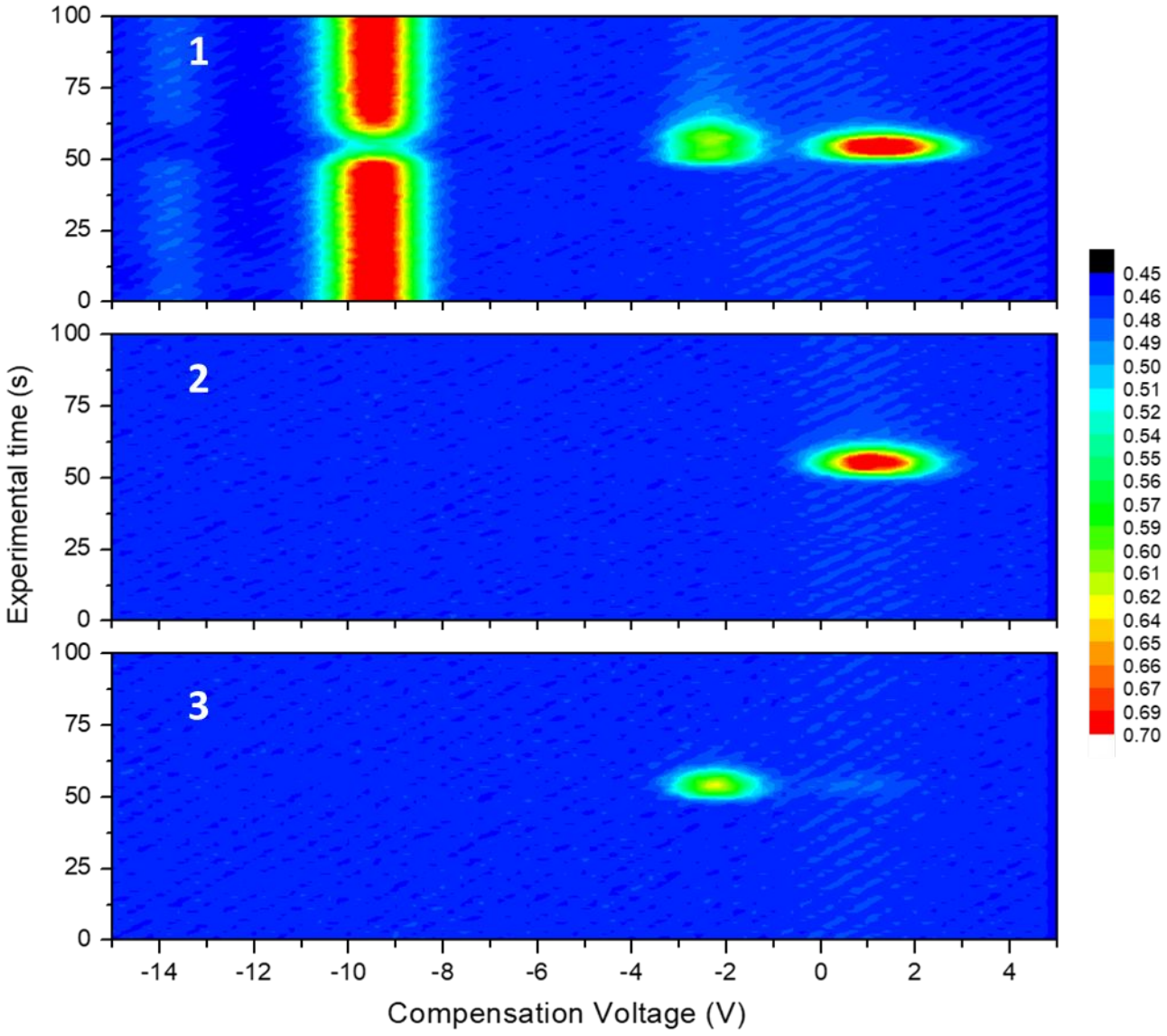

Figure 4. Fowler, et al.

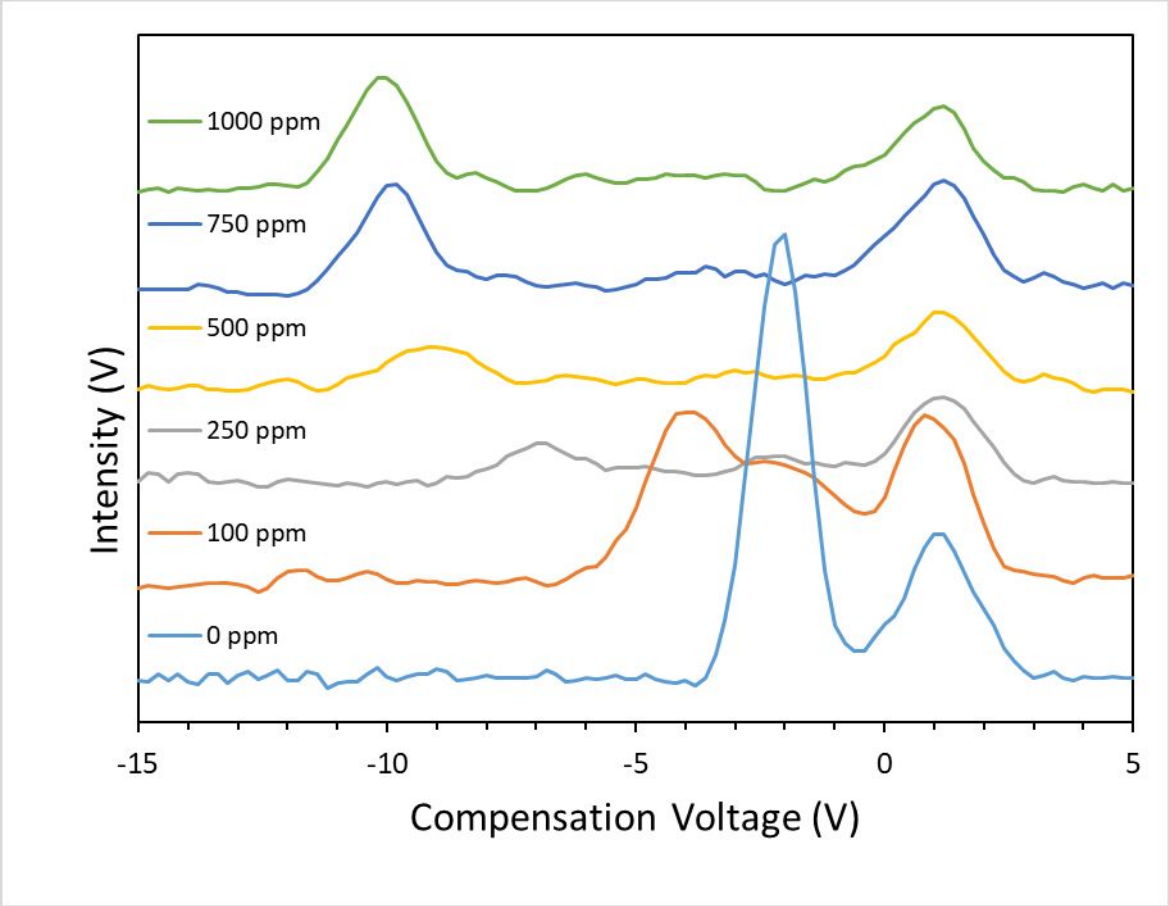

Figure 5. Fowler, et al

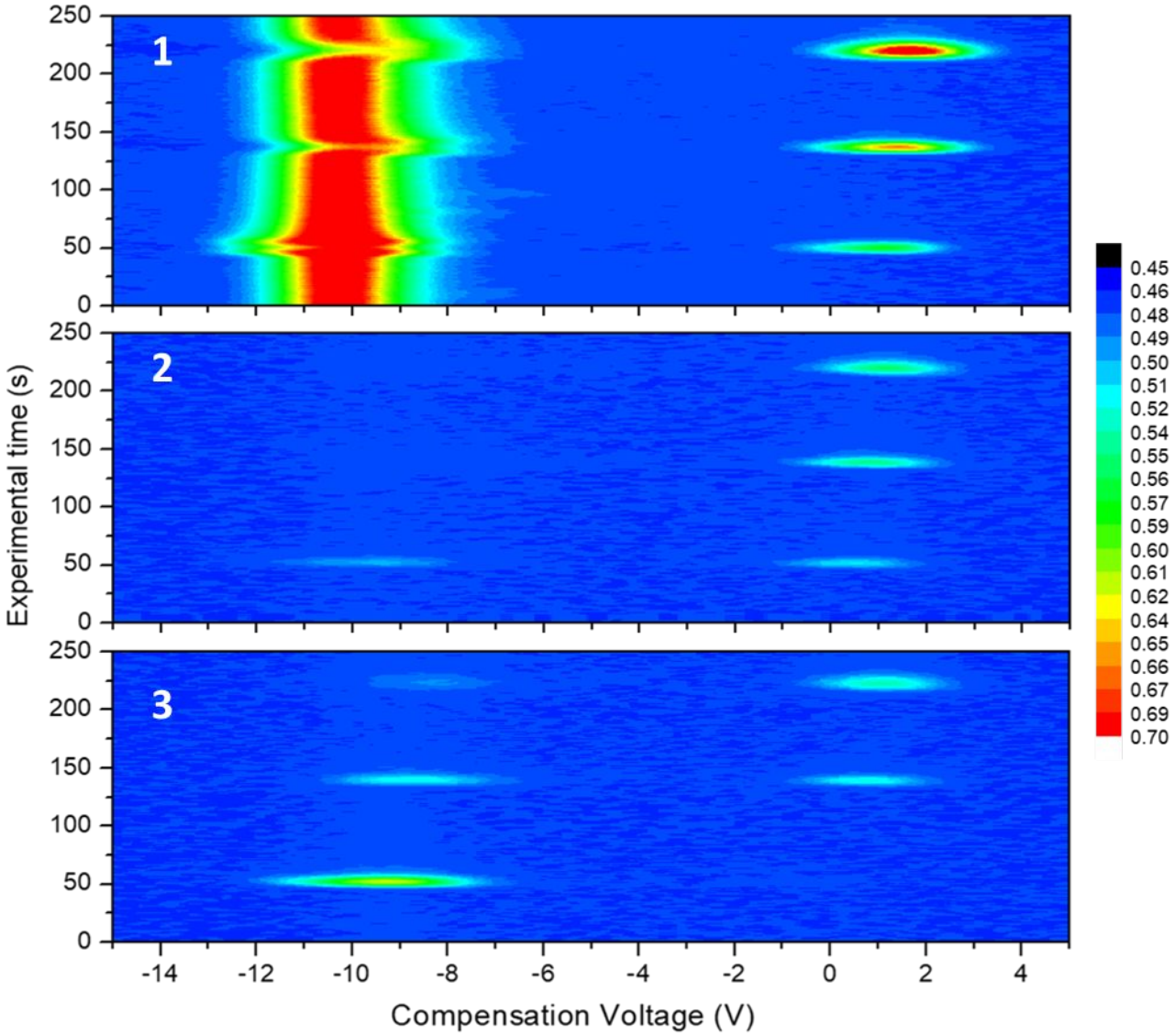

Figure 6. Fowler, et al